AMBIPOLAR DIFFUSION REVISITED

F. C. Adams[1,2]

RESUMEN

Esta contribución reexamina el problema de la difusión ambipolar como un mecanismo para la producción y la evolución fuera de control (colapso) de núcleos en nubes moleculares centralmente condensados. El cálculo principal aplica en el límite geométrico de un núcleo altamente aplanado y permite un tratamiento semi-analítico del problema completo. En esta formulación, el régimen de difusión ambipolar de evolución para tiempos negativos ($t < 0$), se une suavemente a las soluciones de colapso para tiempos positivos ($t > 0$). Este tratamiento muestra que, al final de la época de difusión, los núcleos resultantes tienen velocidades hacia el centro distintas de cero pero submagnetosónicas, de acuerdo con observaciones actuales. Este trabajo deriva una relación analítica entre la razón nodimensional de masa a flujo magnético, $\lambda_0 \equiv f_0^{-1}$, de las regiones centrales producidas por la condensación desbocada y la tasa adimensional de difusión ambipolar, ϵ_0; los núcleos que se colapsan tienen típicamente valores de la razón de masa a flujo, $\lambda_0 \approx 2$. Después mostramos que la difusión ambipolar ocurre más rápidamente en presencia de fluctuaciones turbulentas, i.e., el valor efectivo de la constante de difusión, ϵ_0, puede ser aumentada por la turbulencia. También estudiamos el colapso autosimilar con la inclusión de velocidades iniciales hacia adentro distintas de cero. Estos resultados muestran que la teoría resultante provee un paradigma que funciona para la formación de núcleos en nubes moleculares y su subsecuente colapso para formar estrellas y sistemas planetarios.

ABSTRACT

This contribution re-examines the problem of ambipolar diffusion as a mechanism for the production and runaway evolution (collapse) of centrally condensed molecular cloud cores. The principal calculation applies in the geometric limit of a highly flattened core and allows for a semi-analytic treatment of the full problem. In this formulation, the ambipolar diffusion regime of evolution for negative times ($t < 0$) smoothly matches onto collapse solutions for positive times ($t > 0$). This treatment shows that the resulting cores display non-zero, but sub-magnetosonic, inward velocities at the end of the diffusion epoch, in agreement with current observations. This work derives an analytic relationship between the dimensionless mass to flux ratio $\lambda_0 \equiv f_0^{-1}$ of the central regions produced by runaway core condensation and the dimensionless rate of ambipolar diffusion ϵ; cores going into collapse typically have values of mass-to-flux ratio $\lambda_0 \approx 2$. Next we show that ambipolar diffusion takes place more quickly in the presence of turbulent fluctuations, i.e., the effective value of the diffusion constant ϵ can be enhanced by turbulence. We also study self-similar collapse with the inclusion of nonzero initial inward velocities. Taken together, these findings show that the resulting theory provides a viable working paradigm for the formation of molecular cloud cores and their subsequent collapse to form stars and planetary systems.

Key Words: ISM: magnetic fields — stars: formation

1. INTRODUCTION

Although we have a good working theory for the formation of single, isolated stars (Shu et al. 1987), the picture is not yet complete. Several important generalizations of this theory are the subject of current research, including the possible effects of the background cluster environment on the star formation process and the physical processes through which the circumstellar disks produced during star formation eventually lead to planet formation. How-
ever, one of the most important unresolved issues is the manner in which the pre-collapse initial conditions are determined. This contribution re-examines the process of ambipolar diffusion as a mechanism to drive core formation and hence determine the initial conditions for collapse.

In the standard picture, core formation was considered to proceed through the process of ambipolar diffusion (Shu 1992). In this context, the magnetic field is tied to the molecular gas, but the gas is only weakly ionized. As the magnetic field exerts a force on the gas to resist the inward pull of gravity, the field lines slip outward relative to the mass, and the

[1]Michigan Center for Theoretical Physics, University of Michigan, Ann Arbor, MI 48109, USA (fca@umich.edu).
[2]Astronomy Department, University of Michigan, Ann Arbor, MI 48109, USA.

core material slowly moves inward; eventually, this process forms a centrally concentrated core that is ready for collapse. In the past decade, however, a number of new observations (e.g., see André et al. 2000) suggest that this picture requires some modification. First, the observed ratio of starless cores to those with embedded infrared sources indicates the the core formation process takes place more rapidly than the original estimates of quasi-static ambipolar diffusion (Mestel & Spitzer 1976; Mouschovias 1976; Shu 1983; Nakano 1979, 1984; Lizano & Shu 1989; Basu & Mouschovias 1994; and many others). Second, starless cores are observed to have significant (but always subsonic) initial inward velocities (e.g., Lee et al. 2001; Harvey et al. 2002, Walsh et al. 2004), a finding that suggests that the core formation processes is not completely quasi-static. Third, the observed density profiles of starless cores can now be measured, and they often have extended central regions of constant density (e.g., Alves et al. 2001); as a result, these core more closely resemble Bonnor-Ebert spheres than singular isothermal spheres (note that these latter profiles were often used as the prototypical pre-collapse states, beginning with Shu 1977).

All of the above considerations suggest that the core formation process may be more "dynamic" than considered previously (e.g., in the simplest incarnation of the four stages of star formation put forth in Shu et al. 1987). In this paper, we present the results of three recent studies that show how ambipolar diffusion produces molecular cloud cores in a manner consistent with current observations. In § 2, we present a self-similar semi-analytic model of the ambipolar diffusion process (Adams & Shu 2007, hereafter AS2007). This calculation is complete, in that it shows how the self-similar solutions for core formation match smoothly onto the self-similar solutions for protostellar collapse; in addition, this work shows that the core formation time scale from ambipolar diffusion is consistent with observations, and predicts the observed value of the initial inward velocities. In § 3, we consider the ambipolar diffusion process in the presence of turbulence; in this case, since ambipolar diffusion is essentially a nonlinear diffusion process, turbulent fluctuations act to speed up the core formation rate (Fatuzzo & Adams 2002; Zweibel 2002; see also Nakamura & Li 2005). Given that initial inward velocities are observed, and predicted by theory (§ 2), we construct new infall collapse solutions with nonzero starting velocities in § 4 (Fatuzzo et al. 2004). Finally, we conclude in § 5 with a summary and discussion of our results.

2. AMBIPOLAR DIFFUSION AND THE GRAVOMAGNETO CATASTROPHE

This section presents an overview of the results from AS2007, which provides a new look at the old problem of core formation through ambipolar diffusion. Due to space limitations, this section only outlines the calculation (see the original paper for further detail). The basic evolutionary equations for a flattened, self-gravitating, cloud core of surface density Σ and radial velocity u, threaded by a magnetic field with vertical component B_z, are taken from previous work (see Shu & Li 1997; Li & Shu 1996, 1997). Specifically, the equation of continuity is given by

$$\frac{\partial \Sigma}{\partial t} + \frac{1}{\varpi} \frac{\partial}{\partial \varpi} [\varpi u \Sigma] = 0 \, . \tag{1}$$

The force equation is

$$\frac{\partial u}{\partial t} + u \frac{\partial u}{\partial \varpi} + \frac{a^2}{\Sigma} \frac{\partial}{\partial \varpi} (\Theta \Sigma) = g + \ell \, , \tag{2}$$

where the acceleration produced by self-gravitation plus magnetic tension, $g + \ell$, is given by

$$g + \ell = \frac{1}{\varpi^2 \Sigma} \int_0^\infty K_0(r/\varpi) S(r, \varpi) 2\pi r dr \, , \tag{3}$$

where the source term is given by

$$S(r, \varpi) = -G\Sigma(\varpi)\Sigma(r) + \frac{B_z(\varpi) B_z(r)}{(2\pi)^2} \, , \tag{4}$$

and the kernel K_0 is defined via

$$K_0(q) = \frac{1}{2\pi} \int_0^{2\pi} \frac{(1 - q\cos\varphi)d\varphi}{(1 + q^2 - 2q\cos\varphi)^{3/2}} \, . \tag{5}$$

In equation (2), a is the gaseous isothermal sound speed, and Θ provides the correction for the effects of the magnetic pressure. Finally, the induction equation, which governs the evolution of the vertical component of the magnetic field threading the core in the presence of ambipolar diffusion, takes the form

$$\frac{\partial B_z}{\partial t} + \frac{1}{\varpi} \frac{\partial}{\partial \varpi} [\varpi u B_z] = \frac{1}{\varpi \Sigma} \frac{\partial}{\partial \varpi} \left[\frac{(2z_0)^{1/2}}{2\pi \gamma \mathcal{C}} \frac{\varpi B_z^2 B_\varpi^+}{\Sigma^{1/2}} \right] , \tag{6}$$

where we have defined the radial component of the field at the upper vertical surface of the core by

$$B_\varpi^+ = \frac{1}{\varpi^2} \int_0^\infty K_0(r/\varpi) B_z(r) \, r dr \, . \tag{7}$$

The half-height z_0 appearing in equation (6) is defined by the assumed vertical hydrostatic equilibrium

(AS2007). The quantities γ and $1/\mathcal{C}$ are, respectively, the usual drag coefficient between ions and neutrals and the height-averaged reciprocal coefficient for the ion mass-abundance (see Shu 1992). An attractive feature of this present approach is that we can delay specifying the numerical value of the product $\gamma\mathcal{C}$ until it comes to specifying dimensional scalings appropriate to specific astronomical objects, as long as the combination of parameters given by equation (14) below is a small number compared to unity.

We define the dimensionless ratio λ of mass per unit area to flux per unit area according to

$$\lambda = \frac{2\pi G^{1/2}\Sigma}{B_z}\,. \tag{8}$$

Next we need expressions for Θ and z_0 in terms of λ for a magnetized singular isothermal disk, the form that our inner core approaches asymptotically at the moment of gravomagneto catastrophe. These relations are derived in AS2007. The resulting relationships have the elegance of simplicity, and we assume that the following expressions hold for all times:

$$\Theta = \frac{2+\lambda^2}{1+\lambda^2} \qquad \text{and} \qquad z_0 = \left(\frac{\lambda^2}{1+\lambda^2}\right)\frac{a^2}{\pi G\Sigma}. \tag{9}$$

Combined with equations (1), (2), (6), the relationships (8) and (9) give us a closed set of equations to solve for Σ, u, B_z, λ, Θ, and z_0.

With the form of the magnetic induction equation specified, we now construct a similarity transformation that changes the original description in terms of the variables (ϖ, t) to a description of (x, t); specifically, we use the relations

$$x = \frac{\varpi}{a|t|}, \quad \Sigma(\varpi, t) = \frac{a}{2\pi G|t|}\tilde{\sigma}(x, t)\,, \tag{10}$$

$$u(\varpi, t) = a\tilde{v}(x, t)\,, \quad B_z(\varpi, t) = \frac{a}{G^{1/2}|t|}\tilde{\beta}(x, t)\,.$$

With this formulation, the equation of continuity is given by

$$|t|\frac{\partial\tilde{\sigma}}{\partial t} + \left(1 + x\frac{\partial}{\partial x}\right)\tilde{\sigma} + \frac{1}{x}\frac{\partial}{\partial x}(x\tilde{v}\tilde{\sigma}) = 0\,, \tag{11}$$

and the force equation becomes

$$|t|\frac{\partial\tilde{v}}{\partial t} + (x+\tilde{v})\frac{\partial\tilde{v}}{\partial x} + \frac{1}{\tilde{\sigma}}\frac{\partial}{\partial x}(\Theta\tilde{\sigma}) = \tag{12}$$

$$\int_0^\infty \frac{ydy}{x^2} K_0\left(\frac{y}{x}\right)\tilde{\sigma}(y, t)\left[f(x, t)f(y, t) - 1\right]\,.$$
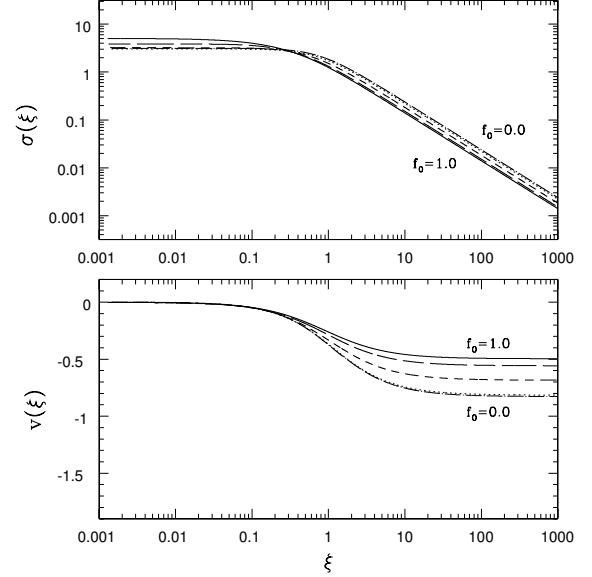
Fig. 1. The dimensionless fluid fields from the self-similar collapse calculation. The top panel shows the reduced density field $\sigma(\xi)$, as a function of the similarity variable ξ, for varying choices of the flux ratio f_0. The bottom panel shows the analogous plot for the reduced velocity field $v(\xi)$.

The induction equation can then be written

$$\tilde{\sigma}^2\left[|t|\frac{\partial f}{\partial t} + (x+\tilde{v})\frac{\partial f}{\partial x}\right] = \frac{\epsilon}{x}\frac{\partial}{\partial x}\left[x\tilde{\sigma}\tilde{b}\left(\frac{f^2}{\sqrt{1+f^2}}\right)\right]\,, \tag{13}$$

where $f \equiv 1/\lambda$ and where we have defined the dimensionless diffusion coefficient

$$\epsilon \equiv \frac{\sqrt{8\pi G}}{\gamma\mathcal{C}}\,. \tag{14}$$

Notice that ϵ is a small dimensionless parameter in this problem, and is essentially the ratio of dynamical time to the diffusion time (see also Galli & Shu 1993). In addition, the reduced radial magnetic field $\tilde{b}$ is defined in terms of the integral

$$\tilde{b}(x, t) = \frac{1}{x^2}\int_0^\infty K_0\left(\frac{y}{x}\right)\tilde{\sigma}(y, t)f(y, t)\,ydy\,. \tag{15}$$

Next, we can eliminate the time dependence from the equations of motion to obtain reduced equations in terms of the variable ξ only (where ξ is a scaled version of x). To carry out this reduction, we must solve for the solution at a given value of the flux ratio $f = f_0$ and then iterate (note that we are omitting several pages of mathematics in this present description — see AS2007 for the full treatment). Figure 1 shows the resulting solutions for the reduced
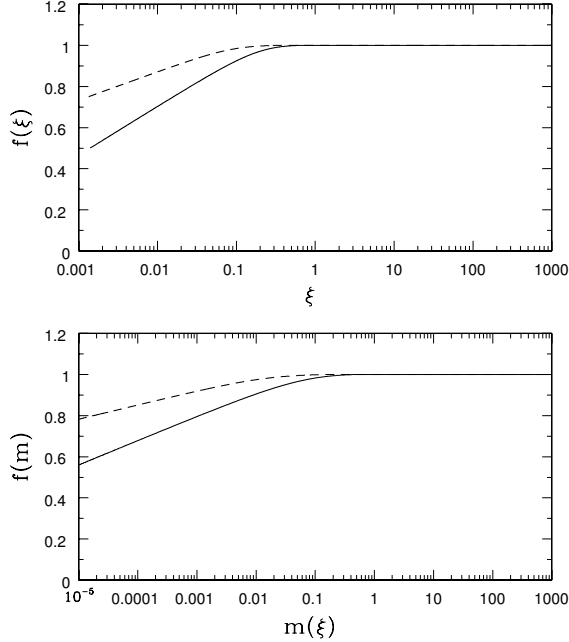
Fig. 2. The flux profile from the self-similar ambipolar diffusion calculation. The top panel shows $f(\xi)$, where ξ is the similarity variable. The bottom panel shows $f(m)$, i.e., the flux ratio as a function of the reduced enclosed mass.

Fig. 3. Self-similar ambipolar diffusion solution for varying times before the moment of collapse. The top panel shows the number density as a function of radius (scaled to typical observed values) for a range of times (as labeled) before the gravomagneto catastrophe. The bottom panel shows the corresponding profiles of inward velocity versus radius for the same times.

fields $\sigma(\xi)$ and $v(\xi)$. Solutions are shown are varying choices of the dimensionless mass to flux ratio f_0. Note that the solutions are nearly independent of the value of f_0. Next, notice that the velocity field always approaches a nonzero value in the limit $\xi \to \infty$, i.e., at large radii in the core (for a given, fixed time). The reduced velocity is given in units of the isothermal sound speed, so these solutions display nonzero, but subsonic, asymptotic inward velocities. The typical value is about half the sound speed, consistent with the observed values in nearby molecular cloud cores (Walsh et al. 2007; Harvey et al. 2002). Notice also that the density and velocity profiles are simple functions and can be fit with simple analytic forms. As result, we have a purely analytic description of the reduced functions, which, when coupled with the original similarity transformation, provide a fully analytic description of the entire epoch of ambipolar diffusion. The corresponding flux profiles are shown in Figure 2. The flux profile approaches the value f_0 at the core center and smoothly matches onto the background cloud so that $f(\xi) \to 1$ in the limit of large ξ.

Figure 3 shows the ambipolar diffusion solution in physical variables (where we have taken the sound speed, etc., to have values typical of nearby clouds

– see AS2007). The time labels denote the time remaining before the gravomagneto catastrophe (the moment that dynamical collapse begins). The bottom panel shows the velocity as a function of radius. As emphasized above, the velocity solution approaches a nonzero, subsonic value in the limit $r \to \infty$. This value, roughly half the sound speed, is consistent with observed values. The top panel shows the density profile as a function of radius, for various times. Two issues are important here: First, at times greater than about 1 Myr before the onset of collapse, the "core" is too spread out to be identified as a molecular cloud core. In these units, the density is less than $n = 10^4$ cm^{-3}, even at the center, which is below the excitation threshold for ammonia. As a result, molecular cloud cores forming via ambipolar diffusion will only be visible as cores for the last $\sim$ 1 Myr before collapse. Second, the core spends relatively more time in its spread out state, with an extended central region at constant density (of relatively low value). The core thus appears much like a Bonnor-Ebert sphere in this phase. In this case, however, the core is not in perfect hydrostatic equilibrium. Instead, the velocity field is nonzero everywhere, and the core becomes increasingly centrally concentrated before it collapses. In other words, Fig-

ure 3 resolves the puzzle of how molecular cloud cores can (often) look like Bonnor-Ebert spheres, but collapse like singular isothermal spheres.

The collapse phase is shown in Figure 4 in physical units. These solutions are much like those found previously (e.g., Shu 1977), with the following modifications: [1] These collapse solutions (valid for $t > 0$) match smoothly onto the ambipolar diffusion solutions (for $t < 0$, Figure 3) across the $t = 0$ boundary (the moment of gravomagneto catastrophe), [2] These solutions display nonzero inward velocities of order 0.1 km/s in the limit $r \to \infty$ (consistent with observations), and [3] The resulting mass infall rates are highly by a factor of about two. The analogous solutions, calculated from the spherically symmetric limit, are outlined in § 4 (see Fatuzzo et al. 2004).

Before leaving this section, we note that this ambipolar diffusion calculation defines a mass scale that can be identified with the characteristic scale for the core mass function. At the moment of gravomagneto catastrophe, the enclosed mass in physical units inside the boundary $\varpi = \varpi_{ce}$ (where the core connects to a common envelope) is given by

$$M_{core} = A \left(\frac{1 + 2f_0^2}{1 - f_0^4} \right) \frac{a^2 \varpi_{ce}}{G}. \qquad (16)$$

Note that the range of allowed flux ratios f_0 is limited. The value of the central flux ratio f_0 is determined by the value of the dimensionless diffusion constant ϵ, where this relationship is explicitly derived in AS2007 (see equation [85] of that paper). In particular, low flux ratios $f_0 < 0.3$ would require $\epsilon > 1$ (which are unphysical in this treatment). For typical values of $a = 0.2$ km/s and $\varpi_{ce} = 0.2$ pc, and for $0.3 \leq f_0 \leq 0.9$, the core masses implied by equation (16) vary from 5 to 22 $M_\odot$. This range in mass scale, a factor of 4.4, is smaller than the observed range of stellar masses. However, the values of a^2 and ϖ_{ce} that specify the mass scale M_{core} can also vary, and the distributions of these parameters add additional width to the resulting distribution of core masses. Moreover, final stellar masses can be appreciably smaller than the core masses at the beginning of dynamical collapse because of various inefficiencies in the star-formation process (e.g., binary formation, stellar winds, bipolar outflows, disk evaporation). These variations will also add width to the distribution of stellar masses (Adams & Fatuzzo 1996). One strength of ambipolar diffusion as a core-formation mechanism is that, given plausible variations of a^2 and ϖ_{ce}, it can produce a core-mass distribution wide enough, when the pivotal state is
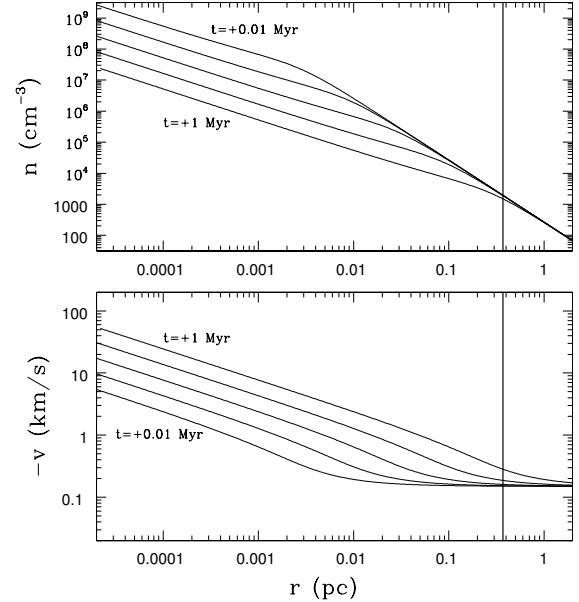
Fig. 4. Self-similar collapse solutions for varying times after the beginning of the collapse phase. The top panel shows the number density as a function of radius (scaled to typical observed values) for a range of times (as labeled) before the gravomagneto catastrophe. The bottom panel shows the corresponding profiles of inward velocity versus radius for the same times.

reached, to span the likely pre-collapse states for making brown dwarfs to high-mass stars.

3. AMBIPOLAR DIFFUSION WITH TURBULENT FLUCTUATIONS

As outlined in the introduction, in the standard paradigm of low mass star formation, molecular cloud cores are supported by magnetic fields, and the cores lose magnetic support through the action of ambipolar diffusion. A critical issue facing this scenario is the time scale required for magnetic support to be removed from the cloud cores. Current observations suggest that the number of cores without stars seems to be smaller than that predicted by estimates from ambipolar diffusion by a factor of 3–10 (e.g., compare Jijina et al. 1999 with Shu 1983), so that the loss of magnetic support by diffusion appears to be too slow. As shown in the previous section (Figure 3), cores are only observable for the last ~ 1 Myr before collapse, so this time scale issue is not as severe as previously reported. In addition, previous calculations have neglected the effects of fluctuations on ambipolar diffusion. Recent work (Fatuzzo & Adams 2002; Zweibel 2002) shows that ambipolar diffusion occurs more rapidly in the presence of fluctuations. In addition, because
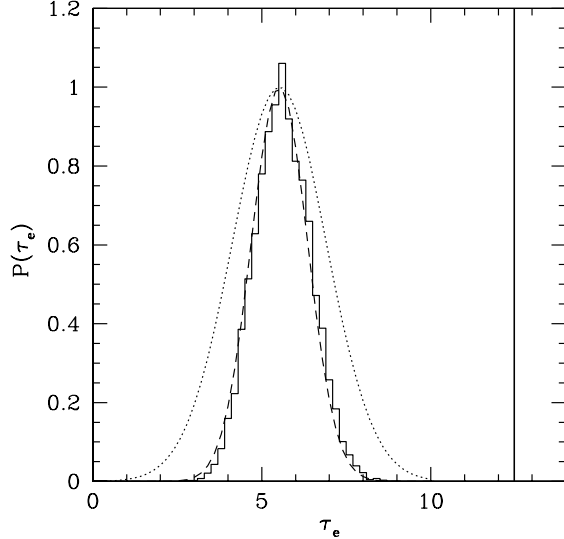
Fig. 5. Distribution of time scales for core formation through ambipolar diffusion in the presence of turbulent fluctuations. The histogram shows the results of 10,000 numerical simulations of the ambipolar diffusion process with different realizations of the fluctuations. The smooth dashed curve shows the analytically predicted distribution for the given level of turbulence; the dotted curve shows the wider distribution that would result with a longer time scale for producing independent realizations of the turbulence. The vertical line on the right hand side of the plot shows the (single) value of the time scale for no turbulent fluctuations.

of the chaotic nature of the fluctuations, the ambipolar diffusion time scale will take on a full distribution of values for effectively "the same" initial states.

Fluctuations in both the magnetic field strength and the density field are expected to be present in essentially all star forming regions. Molecular clouds are observed to have substantial non-thermal contributions to the observed molecular line-widths; these non-thermal motions are generally interpreted as arising from MHD turbulence. Indeed, the size of these non-thermal motions, as indicated by the observed line-widths, are consistent with the magnitude of the Alfvén speed. As a result, the fluctuations are often comparable in magnitude to the mean values of the fields (in other words, the relative amplitudes of the fluctuations are of order unity).

Background fluctuations can lead to a net change in the diffusion rate because magnetic diffusion is a nonlinear process. As many authors have derived previously (e.g., Shu 1992), the dimensionless diffusion equation takes the schematic form

$$\frac{\partial b}{\partial \tau} = \frac{\partial}{\partial \mu}\left(b^2 \frac{\partial b}{\partial \mu}\right), \qquad (17)$$

where b is the magnetic field strength, μ is the Lagrangian mass coordinate, and we have ignored density variations. If the magnetic field fluctuates about its mean value on a time scale that is short compared to the diffusion time, then we let $b \to b(1+\eta)$, where η is the relative fluctuation amplitude. In the simplest case where the fluctuations are spatially independent, the right hand side of equation is multiplied by a cubic factor $(1+\eta)^3$. Although a linear correction would average out over time, this nonlinear term averages to a value greater than unity, and the corresponding diffusion time scale grows shorter.

We have derived a more rigorous treatment of this effect by including both magnetic field and density fluctuations (Fatuzzo & Adams 2002) into the standard one-dimensional ambipolar diffusion problem (Shu 1983, 1992). For the case of long wavelength fluctuations, the rate of ambipolar diffusion increases by a significant factor $\Lambda \sim 1-10$. The corresponding decrease in the magnetic diffusion time helps make ambipolar diffusion more consistent with observations. In addition, the stochastic nature of the process makes the ambipolar diffusion time take on a distribution of different values.

Figure 5 shows the resulting distribution of ambipolar diffusion times for a cloud layer with uniform fluctuations of amplitude $A = 0.886$; this level of fluctuations is consistent with the non-thermal line widths observed in star forming regions. The solid curve (histogram) shows the result of 10,000 numerical simulations with different realizations of the fluctuations. The dashed curve shows the analytic prediction for the time scale distribution – a gaussian with a peak value given by the expectation value and with a width predicted by application of the central limit theorem. The dotted curve depicts a wider gaussian distribution that applies for longer fluctuation time scales (resulting in fewer realizations of the turbulent fluctuations). In the absence of fluctuations, the cloud maintains a single value for its ambipolar diffusion time, as shown by the delta-function spike at $\tau_e \approx 12.5$.

4. GENERALIZED SELF-SIMILAR COLLAPSE

Motivated by recent observations that show starless molecular cloud cores exhibit subsonic inward velocities, we revisit the collapse problem for polytropic gaseous spheres. In particular, we provide a generalized treatment of protostellar collapse in the spherical limit (Fatuzzo et al. 2004) and find semi-analytic (self-similar) solutions, corresponding numerical solutions, and purely analytic calculations of the mass infall rates (the three approaches are in
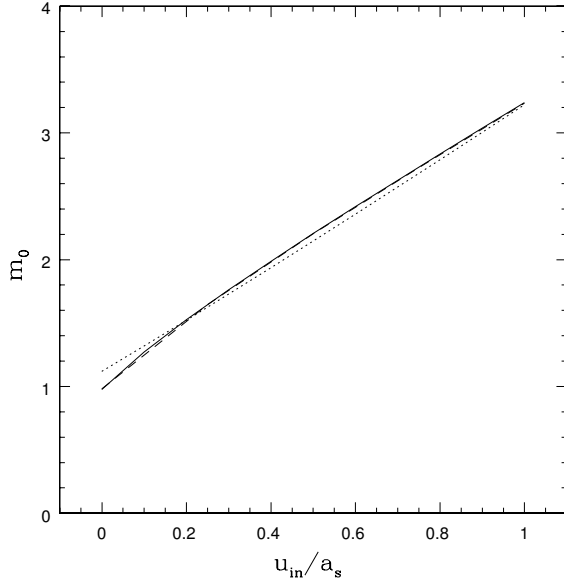
Fig. 6. Comparison of self-similar, analytic, and numerical determinations of m_0 for varying initial inward velocities u_{in} and for isothermal initial conditions. The m_0 values calculated from the self-similar equations of motion (solid curve), numerically solving the partial differential equations (dashed curve), and an analytic estimate (dotted curve). All models use initial states with isothermal static $\Gamma = 1$ and dynamic $\gamma = 1$.

good agreement). This study focuses on collapse solutions that exhibit nonzero inward velocities at large radii, as observed in molecular cloud cores, and extends previous work in four ways: (1) The initial conditions allow nonzero initial inward velocity. (2) The starting states can exceed the density of hydrostatic equilibrium so that the collapse itself can provide the observed inward motions. (3) We consider different equations of state, especially those that are softer than isothermal. (4) We consider dynamic equations of state that are different from the effective equation of state that produces the initial density distribution. This work determines the infall rates over a wide range of parameter space, as characterized by four variables: the initial inward velocity u_{in}, the overdensity Λ of the initial state, the index Γ of the static equation of state, and the index γ of the dynamic equation of state. For the range of parameter space applicable to observed cores, the resulting infall rate is about a factor of two larger than found in previous theoretical studies (those with hydrostatic initial conditions and $u_{in} = 0$).

This work allows for a greater understanding of the infall rate $\dot{M}$, which is perhaps the most important variable in the star formation problem. For
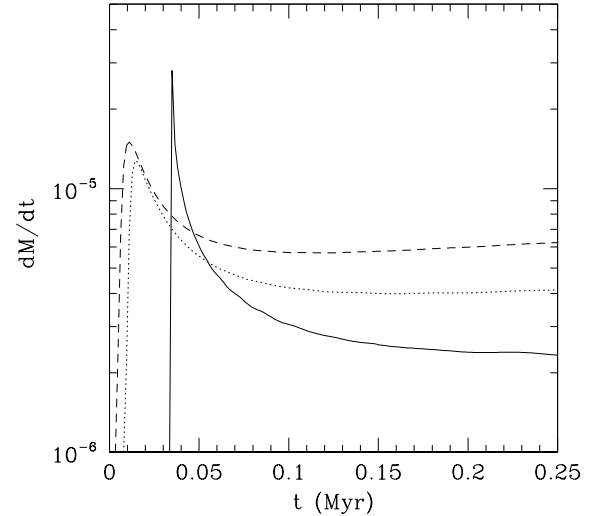
Fig. 7. Mass infall rates as a function of time for flat-topped cores. The initial (asymptotic) inward velocities are taken to be $u_{in} = 0$ (solid curve), 0.5 a_S (dotted curve), and 1.0 a_S (dashed curve).

isothermal initial conditions, the mass infall rate is given by $\dot{M} = m_0 a_s^3/G$ so that the dimensionless parameter m_0 specifies the infall rate. For example, Figure 6 shows the values of m_0 calculated using three different approaches: the "standard" self-similar formulation (as in Shu 1977), an analytic estimate, and a fully numerical determinations. The resulting values of m_0 are shown as a function of the initial inward velocity. All of these cases use initial states with isothermal static $\Gamma = 1$ and dynamic $\gamma = 1$. Notice that the three approaches are in good agreement, and that the infall rate is a smoothly increasing function of the initial velocity. For observed values of u_{in}, the infall rate is roughly twice the canonical value (for hydrostatic initial conditions).

Figure 7 shows the mass infall rates as a function of time for flat-topped cores with varying infall speeds. This set of numerical collapse calculations begins with typical parameters observed in flat-topped cores with sound speed $a_S = 0.2$ km/s, and assumes a central region of nearly constant density spanning $r_C \approx 10^{16}$ cm. The initial states are taken to be overdense at the 10 percent level. The solid curve shows the resulting mass infall rate (expressed in $M_\odot$ yr^{-1}) for the case with no initial velocity. The dotted (dashed) curve shows the corresponding mass infall rate for starting inward speeds of $u_{in} = 0.5$ a_S ($u_{in} = a_S$). When $u_{in} \neq 0$, the mass infall rates reach their peak values more quickly, the peak values are smaller, and the infall rates more rapidly approach their asymptotic values (as predicted by

the similarity solutions). Thus, for the case of $u_{in} = 0.5\, a_S$ (roughly the observed value), the infall rate shows a moderate peak at early times (consistent with observed spectral energy distributions of Class 0 sources) and a later plateau (consistent with Class I sources).

5. CONCLUSION

In this paper, we have reviewed the case for ambipolar diffusion as a mechanism for producing molecular cloud cores and thus determining the initial conditions for protostellar collapse. We have presented a self-similar formulation of the problem (§ 2, AS2007) that provides a complete solution, including the ambipolar diffusion epoch for $t < 0$ and the collapse phase for $t > 0$ (Figures 3 and 4). These solutions match smoothly across the $t = 0$ boundary, which represents the moment that collapse begins, and is known here as the gravomagneto catastrophe. This updated treatment of ambipolar diffusion shows that the time scale for which cores can be observed as cores is relatively short, ~ 1 Myr, roughly consistent with observations of core statistics (e.g., Jijina et al. 1999). Moreover, the cores spend most of their pre-collapse phase with an extended region of nearly constant density, so they resemble Bonnor-Ebert spheres for much of their evolution (as observed, e.g., Alves et al. 2001). However, the cores are not Bonnor-Ebert spheres, as they are not hydrostatic, but rather are condensing into centrally concentrated states, with a characteristic inward velocity (at large radii) of about half the sound speed, given both by observations (e.g., Lee et al. 2001) and by the theory of § 2 (AS2007). This process also defines a mass scale (equation 16) that can be made consistent with observed core mass functions (e.g., Lada et al. 2008), for both the characteristic mass and width of the distribution.

The core formation time scale can be reduced further through the action of turbulent fluctuations (§ 3; Fatuzzo & Adams 2002; Zweibel 2002). The inclusion of fluctuations not only speeds up the ambipolar diffusion rate, but it also implies that the core formation time will be sampled from a distribution of values (Figure 5), i.e., the formation time scale depends on the particular realization of the fluctuations (which vary from case to case). For completeness, this paper has also reviewed recent generalizations of the infall-collapse solutions (§ 4; Fatuzzo et al. 2004). This work shows that the initial inward velocities increase the mass infall rate compared to the case of hydrostatic initial conditions; the observed asymptotic velocities $u_{in} \sim 0.1$ km/s imply a factor

of two increase in $\dot{M}$. Finally, for $u_{in} \neq 0$, the mass infall rate for flat-topped cores is more nearly constant in time, compared with the hydrostatic case (Figure 7).

Given the results outlined above, this updated treatment of ambipolar diffusion is consistent with observed core formation time scales, observed core density profiles, observed asymptotic inward velocities, and observed core mass functions. Further, the subsequent collapse properties are consistent with our current understanding of Class 0 and Class I protostellar sources. Ambipolar diffusion thus provides a viable mechanism to drive the formation of molecular cloud cores and thereby determine the initial conditions for star formation.

REFERENCES

Adams, F. C., & Fatuzzo, M. 1996, ApJ, 464, 256
Adams, F. C., & Shu, F. H. 2007, ApJ, 671, 497 (AS2007)
Alves, J. F., Lada, C. J., & Lada, E. 2001, Nature, 409, 159
Andŕe, P., Ward-Thompson, D., & Barsony, M. 2000, in Protostars and Planets IV, eds. V. Mannings, A. Boss, & S. Russell (Tucson: Univ. Arizona Press), 59
Basu, S., & Mouschovias, T. Ch. 1994, ApJ, 432, 720
Fatuzzo, M., & Adams, F. C. 2002, ApJ, 570, 210
Fatuzzo, M., Adams, F. C., & Myers, P. C. 2004, ApJ, 615, 813
Galli, D., & Shu, F. H. 1993, ApJ, 417, 220
Harvey, D. W. A., Wilner, D. J., DiFrancesco, J., Lee, C. W., Myers, P. C., & Williams, J. P. 2002, AJ, 123, 3325
Jijina, J., Myers, P. C., & Adams, F. C. 1999, ApJS, 125, 161
Lada, C. J., Muench, A. A., Rathborne, J., Alves, J. F., & Lombardi, M. 2008, ApJ, 672, 410
Lee, C. W., Myers, P. C., & Tafalla, M. 2001, ApJS, 136, 703
Li, Z.-Y., & Shu, F. H. 1996, ApJ, 472, 211
_____. 1997, ApJ, 475, 237
Lizano, S., & Shu, F. H. 1989, ApJ, 342, 834
Mestel, L., & Spitzer, L. 1956, MNRAS, 116, 505
Mouschovias, T. Ch. 1976, ApJ, 207, 141
Nakamura, F., & Li, Z.-Y. 2005, ApJ, 631, 411
Nakano, T. 1979, PASJ, 31, 697
_____. 1984, Fund. Cosmic Phys., 9, 139
Shu, F. H. 1977, ApJ, 214, 488
_____. 1983, ApJ, 273, 202
_____. 1992, Gas Dynamics (Mill Valley: Univ. Science Books)
Shu, F. H., Adams, F. C., & Lizano, S. 1987, ARA&A, 25, 23
Shu, F. H., & Li, Z.-Y. 1997, ApJ, 475, 251
Walsh, A. J., Myers, P. C,. & Burton, M. G. 2004, ApJ, 614, 194
Zweibel, E. 2002, ApJ, 567, 962